# The Effect of Deliberate Aluminium Additions on the Microstructure of Rolled Steel Plate characterized using EBSD

Y. Palizdar[1], R. C. Cochrane[1], R. Brydson[1], D. Crowther[2], D. San Martin[3] and A. J. Scott[1]

preyp@leeds.ac.uk

Tel and Fax: +441133432552

[1]Institute for Materials Research, SPEME, University of Leeds, Leeds LS2 9JT UK

[2]Corus Group, Swinden Technology Centre, Rotherham, S60 3AR UK

[3]MATERALIA group, Department of Physical Metallurgy, (CENIM-CSIC), Centro Nacional de Investigaciones Metalúrgicas Av. Gregorio del Amo 8, 20040 Madrid, Spain.

**Key words**: low carbon steel, aluminium, ferrite grain size, EBSD

The use of aluminium as a deliberate alloying addition in steels has attracted increased attention recently as a possible replacement for Si in Transformation Induced Plasticity (TRIP) steels. In addition, some authors have suggested that it offers beneficial effects as a solid solution strengthener as well as galvanizability. In this work three low carbon (0.02 wt%) manganese (1.4 wt%) steels have been alloyed with very different aluminium contents (0.02, 0.48 and 0.94 wt%) in order to study the effect of this alloying element on the final ferritic microstructure. Two different rolling schedules have been applied to these steels and the final microstructures have been characterized extensively by EBSD measurements. The results indicate that aluminium additions have a profound influence on ferrite grain size and the grain boundary misorientation distribution functions.

## 1. Introduction

Traditionally, aluminium has been used in steels mainly as a deoxidising or grain refining element (combined with nitrogen it forms AlN precipitates that inhibit austenite grain growth) in amounts rarely exceeding 0.01 to 0.07 wt%, except in specialized steels for nitriding or forging applications. At present there is a great commercial interest in Al additions, of the order of 0.5-2 wt%, to low carbon, high strength strip steels to produce a highly desirable multi-phase microstructure containing retained austenite for cold forming applications for which a coarse grained ferritic structure is preferred. These steels rely on conventional strip mill processing to produce a microstructure composed of ferrite, austenite, bainite and martensite which possesses a combination of high strength and ductility. Such good properties originate from the so-called transformation-induced plasticity (TRIP) effect, which arises due to the transformation of austenite to martensite during plastic deformation [1-3]. However, inappropriate processing of such steels is known to produce a ferrite/martensite microstructure with very poor formability behaviour and toughness. In addition, recently Mintz [4] has shown that Al additions can be used as a solid solution strengthener.

Apart from the effect of additional Al on the mechanical properties of TRIP steels and also the effect of AlN on steel microstructure, there is very little detailed literature concerning the effect of aluminium in amounts higher than 0.1 wt% on steel microstructure. Aaronson and co-workers [5] showed that additional aluminium in amounts of 1.5 wt% increases the $Ae_3$ temperature (austenite to ferrite transition temperature). Also, Mabuchi et al. have shown that the addition of aluminium can change the steel microstructure [6, 7] from mostly fine ferrite to coarse upper bainite in a Mn-Mo steel. Nakamaya [8] has studied the effect of aluminium on the grain size of a magnetic steel and Jeong [9] has investigated the role of aluminium in an ultra low carbon steel. Both studies indicated that aluminium has a pronounced effect on the ferrite grain size present in the final microstructure. Thus, although there has been some work on the effect of aluminium in steel microstructures, it is believed that there has been no comprehensive study about the effect of free aluminium in steel, particularly in amounts ranging between 0.1 wt% and 1.5 wt%, on the final ferritic microstructures and ferrite transformation kinetics.

Following our previous work [10, 11] on the effect of Al in steels with the same base composition (0.02 C wt% - 1.5 Mn wt%) and different aluminium contents (0.02, 0.48 and 0.94 wt%), in this work the ferritic microstructures obtained in these steels, following two different rolling schedules, is characterized extensively. The average ferrite grain size, ferrite grain size distribution and misorientation distribution function have been analyzed in the mid-thickness, central region of rolled plates using electron backscattered electron diffraction (EBSD). This technique has allowed us to obtain detailed microstructural information that would either not be obtainable or would take a significantly longer time using other techniques such as XRD, TEM and/or optical microscopy.

## 2. Materials and Methods

To investigate the influence of aluminium on steel microstructure, three low carbon steels with a range of aluminium additions (0.02, 0.48, 0.96 wt% Al) were prepared in a laboratory vacuum melt furnace as 50kg casts. Table 1 shows the chemical compositions for each steel. As can be seen, the level of nitrogen was kept as low as possible so as to avoid the formation of aluminium nitride precipitates (which would complicate any analysis of the effect of free aluminium on microstructure). Besides the composition, Table 1 also shows the expected amount of free Al in solid solution, assuming that all the nitrogen in the steel is combined with aluminium, forming AlN precipitates. The amount of free Al can be estimated using the following equation[7]:

$$\text{Al (free)} = \text{total Al} - 27/14\ \text{N} \quad \text{(in wt\%)} \qquad (1)$$

To investigate the size and quantity of AlN precipitates, carbon replicas were extracted and analyzed by transmission electron microscopy (TEM) using a Philips CM20 TEM operated at 200 kV

Two different schedules were used to study the effect of rolling on the final ferritic microstructure (Table 2). These schedules were based on previous experience of laboratory rolling of C-Mn-Nb steels and, as such, were not expected to be optimal for these low carbon steels. The first rolling schedule, hot rolling (HR), consisted of rolling the plate from 1250 $^{o}$C continuously down to a finish rolling temperature (FRT) of ~1090 $^{o}$C; this contrasts with the second schedule, controlled rolling (CR), which used the same reductions per pass but with an intermediate hold at 42 mm plate thickness during which time the temperature dropped from ~1180 $^{o}$C to ~1050 $^{o}$C, rolling then continued (with the same reductions per pass) down to a lower FRT of 950 $^{o}$C. Surface temperatures at the start and end of rolling were measured by a pyrometer approximately 1 m above the exit of the rolling stand and are not considered particularly reliable; the temperatures quoted here are based on implanted thermocouple measurement on the rolling mill at Corus STC Rotherham and backed up by computer modelling of the time/temperature profile for plates of similar dimensions rolled on the same mill [12].

The metallography specimens were polished and etched with 2% nital. The specimens were examined using a Nikon Optiphot reflected light microscope. Images were captured from the centre of specimens using a CCD camera and Zeiss Axiovision software.

To assess the average ferrite grain size and ferrite grain size distribution for each steel, EBSD measurements were employed. Samples were prepared by polishing on a Buehler Vibromat vibratory polisher using non-crystallising colloidal silica. EBSD measurements were carried out using a Carl Zeiss SMT Leo 1530 FEG-SEM operated at 30 kV with patterns detected and analysed in real time using an Oxford Instruments camera and associated INCA software. EBSD maps were collected for each sample from the middle of each plate using a step size of approximately 1 μm and a 5 degree misorientation cut off was applied for the purposes of identifying individual grains. To enhance the reliability of the results, EBSD measurements were performed at low magnification in order to include a sufficient number of grains (in general, more than 600 grains).

## 3. Results

The metallography images of samples E, F, G (HR) and L, M (CR) are shown in Figure 1. Figure 2 shows the EBSD grain orientation maps for each sample. Table 3 shows the average ferrite grain size obtained by EBSD. The mean linear intercept values were calculated from the ASTM numbers determined by the EBSD software. As can be seen, for the same rolling schedule (HR or CR), increasing Al content leads to a finer ferritic microstructure. As has been reported previously [10], the additional Al in the HR condition does not cause a significant change in ferritic microstructure when present in amounts less than 0.5 wt%, however, the present study on the CR condition shows that a change in ferrite grain size is apparent in this condition when Al is present at levels of ~0.5 wt%. Although a finer grain structure was expected in the CR as opposed to the HR condition, comparison between steels E and L (both containing 0.02 wt% Al) shows no appreciable difference. However, in Al treated steels (F and M both containing 0.48 wt% Al) a considerable reduction in ferrite grain size can be observed for the CR condition.

Figure 3 compares the ferrite grain area distributions for the investigated steels. As explained recently [10], comparison of the ferrite grain area distribution (FGAD) for steels E and F shows little change while the FGAD for composition G shows a narrower and tighter distribution. Apparently, there are finer ferrite grains present in G and the additional Al has eliminated all grains coarser than 3200 $\mu m^2$. Figure 3b shows the influence of additional Al in the CR condition. The FGAD for M shows a much higher number of small ferrite grains. For instance, for steel M in Figure. 3b, 45% of the grains are less than 600 $\mu m^2$ in area while there is a much wider range of grain areas for steel L. In contrast, the FGAD of steel L shows a long tail of large grains, hence there is a greater percentage of the overall area fraction in the form of grains coarser than 4400 $\mu m^2$. A comparison of steels F and M (Figure 3a and 3b) indicates that in the CR condition, as expected, much finer grains can be observed and coarse grains are scarce.

The previous grain misorientation distributions results (HR) [10] have been compared with the results from CR condition in Figures 4a and 4b. The dashed line shows the theoretical distribution for randomly oriented grains provided by Mackenzie [13]. Although the grain misorientation distributions for steels E and F (Figure 4a) are qualitatively similar to that predicted for a completely random orientation of grains, the results do reveal that there is a high proportion of low angle misorientations, particularly for the Al-containing steels G (0.94 wt% Al and HR) and control rolled steels.

The presence of any AlN particles, which could lead to grain refinement, was determined via TEM for both Al treated, hot rolled samples (F and G). TEM results show that the AlN particle size extracted by the carbon replica technique to be approximately 500 nm (Figures 5a and 5b).

## 4. Discussion:

**4.1** Ferrite grain size

As mentioned before, there is little in the literature concerning the effect of Al as a solute element on ferrite grain size. However, there is some work concerning the effect of additional Al up to 0.3-0.4 wt %, mostly in high Si magnetic steels. In these afore-mentioned studies, attempts were made to reveal the effect of Al in the range of 0.001-0.4 wt% on ferrite grain size. These studies concluded that the effect of Al on ferrite grain size can be categorized as follows:

1) The effect of Al in amounts between 0.01-0.07 wt%; here, the effect of Al as a grain refiner element has been well established [14]. It is well known that Al can form AlN and inhibit both austenite and ferrite grain growth. This means that by adding Al to a nitrogen containing steel (commercial steels normally contain between 0.002 and 0.008 wt% N) a finer ferrite grain size can be obtained.

2) The effect of Al at higher amounts (> 0.07 wt%); there is little in the literature concerning Al additions above 0.07 wt % which is expected since there is no desire by steel makers to produce high Al steels owing to the fact that high Al content can cause lower castability with problems such as nozzle blocking. Also, since Al has not been recognized as a solid solution strengthener there was no reason for steel makers to use Al as a deliberate addition to steels except as noted in the introduction. However, information about the effect of additional Al in amounts between 0.1-0.4 wt% can be found [8, 9, 15, 16]. Nakamaya and Hojou have shown that by adding 0.07 wt% Al, ferrite grains become finer while the addition of more than 0.1 wt% Al leads to

slightly coarser ferrite grains as compared with the Al free steel [8]. They attributed this phenomenon to the effect of additional Al on the size of AlN particles. As they reported, adding more Al to the steel makes the AlN particles coarser. For instance, in a 0.05 wt %Al steel the average AlN particle size observed was 50 nm while in a 0.3 wt % Al steel AlN particles up to 1.2 μm were seen. It is well established in the literature [14] that by increasing the size of AlN, these particles lose their efficiency in contributing to the grain boundary pinning process.

In addition to the role of AlN in controlling ferrite grain size in Al-treated steels (in amounts higher than 0.1 wt%), there are two more factors which need to be considered. These are the effect of Al on the prior austenite grain size, not only as a result of the presence of AlN particles but also, more directly, Al segregation to austenite grain boundaries causing solute drag, and the influence of Al on critical transformation temperature ($Ae_1$, $Ae_3$ ). It is believed that in steels with high Al contents, for example 0.5 wt% or more, these two latter factors play important roles. However, these parameters have been ignored in the mentioned studies.

Concerning the role of AlN in the investigated steels, our TEM results (Figure. 5) are consistent with the previous results of Nakamaya and Saxena [8, 16]. As can be seen, AlN particles in steels F and G are observed to be around 500 nm in size. This, together with the fact that there is no significant difference in the volume fraction of AlN in steels E, F and G, due to the very low levels of N, it is believed that the limited number of relatively large AlN particles do not play a significant role in the determination of the final ferrite grain size.

Alternative interpretations for the appearance of finer ferrite grains in Al containing steels may be associated with the effect of Al on the $Ae_3$ temperature and also on the accumulated strain prior to the austenite to ferrite transformation. The critical transformation temperatures for the investigated steels were determined by using dilatometry and reported in a previous paper [10]. However, the authors believe that the application of a very low heating rate enables Al atoms to partition into ferrite which would automatically raise the measured $Ae_3$. It is considered that transformation during rolling would take place rapidly at relatively fast cooling rates and therefore there is little prospect for Al partitioning to transforming ferrite austenite interfaces. Calculation of transformation non-partition temperatures using MTData [17] was performed to obtain a better understanding of the results. Table 4 shows the $Ae_1$ and $Ae_3$ temperatures predicted by MTData for steels E, F and G; it can be assumed temperatures $Ae_1$ and $Ae_3$ for steels L, M are the same as those predicted for steels E and F. Many studies of controlled rolling have shown that the amount of retained strain in austenite plays a significant role in the determination of the final ferrite grain size that is observed at the end of rolling [18]. The MTData results show that additional Al can raise the $Ae_3$ temperature and hence the FRT moves closer to $Ae_3$ in the Al treated steels (F and G). In addition, increasing the $Ae_3$ leads to there being less time for austenite grain growth after finishing the rolling. Therefore, during the cooling after rolling in the higher Al content steels, austenite grains will have less time to recrystallize and grow before commencing the austenite to ferrite phase transformation and therefore the ferrite grain size can be expected to be smaller for steel G as compared to steels F or E. A combination of all these phenomena would lead to a finer ferrite grain structure. However, more structured rolling studies would be needed in order to fully understand the whole process.

In addition, the CR samples show a more pronounced effect of additional Al on ferrite grain size in comparison with the HR samples. However, changes in the rolling schedule do not appear to have the same influence for the 0.02 wt% and 0.5 wt% Al containing steels. The results show that control rolling of the 0.02 wt % Al steel leads to a slightly coarser average ferrite grain size and also promotes the presence of very large ferrite grains (Figure 3b). A likely explanation for the reason why steel L was coarser grained after an apparently more 'controlled' rolling schedule (compare with steel E) lies in the rolling schedule used. As already mentioned, the particular rolling schedule used here for CR had not been optimized for the controlled rolling of steels with such low C contents (being based on studies of Nb steels with carbon contents from 0.05 to 0.15 wt%). During the early development of controlled rolling practices, it has been well documented that the controlled rolling process would not lead to a desirable microstructure unless austenite recrystallisation is properly controlled before the plate temperature falls into the partial recrystallisation region [19, 20]. It is highly probable that in the absence of any effective pinning particle such as AlN, the growth rate of austenite grains would become extremely high. Therefore, holding the material at 1180 ºC and allowing it to fall to 1050 ºC allows the development of some coarse austenite grains which subsequently give rise to coarse grains of ferrite. The appearance of ferrite grains greater than ~5000 $\mu m^2$ (Figure 3b) is consistent with this interpretation.

As mentioned above, the effect of additional Al on ferrite grain size is considerably more in the CR condition (steel M). The interpretation of more pronounced grain refinement in the CR condition could be due to the lower FRT (in comparison with steel F) which results in higher retained strain and less time for growth and also the effect of Al on prior austenite grain size which could lead to noticeable grain refining.

**4.2** Ferrite grain misorientation distribution (GMOD)

Regarding the change in the grain misorientation distribution (GMOD) it should be noticed that there appears to be a correlation between a higher number of low angle misorientations and the levels of additional Al in the steel and also controlled rolling ( Figures 4a and 4b, respectively). The presence of excess low angle grain boundaries i.e. $< 15^{\circ}$ has been reported in some cases [21, 22]. Priestner and Ibraheem [21] have shown that warm rolling of a Nb steel results in an excess of low angle grain boundaries which are representative of substructure. Table 5 and Figure 6 show considerable correlation between the amount of low angle grain boundaries and difference between $Ae_3$ and FRT for each steel. In the case of our investigated steels it is believed that when $Ae_3$ becomes close to the finishing rolling temperature (FRT) the amount of low angle grain boundaries raises. For instance, a comparison among E, F and G shows that the steel which has the higher $Ae_3$ has a higher excess of low angle misorientations. Also, a similar effect is seen for the CR condition. However, it should be noted that comparison between HR and CR grain boundary misorientation distribution (GBMD) results shows that in general CR steels have a greater proportion of low angle boundaries which can be interpreted as a consequence of lower FRT for this specific type of rolling schedule or in other words, a lower difference between $Ae_3$ and FRT.

Generally, the CR results are consistent with our previous observations on the HR steels and also with those of Priestner and Ibraheem [21]. However, it should be noted that they observed a higher proportion of low angle grain boundaries owing to the specific type of rolling schedule.

## 5. Conclusion

The results presented here show the strong effect of significant Al additions to ultra-low carbon and nitrogen steels on ferrite grain size. Both the level of nitrogen present in the steels plus TEM observations, lead us to believe that this can not arise as a consequence of AlN formation. We suggest that this grain refinement should be considered to be mainly an effect of aluminium on the $Ae_3$ temperature and, consequently, the amount of retained strain in austenite. The other interesting result which needs further consideration is the presence of low grain misorientation angles in Al-containing steels. These results show that the existence of excess low angle grain boundaries not only in Al treated steels but also high levels in those Al containing steels which had undergone controlled rolling. Also, these results can be interpreted as an influence of Al on $Ae_3$ which leads to a smaller difference between the FRT and $Ae_3$.

**Reference**:


[1] S. C. Baik, S. H. Park, H. Kwon, D. I. Kim, K. H. Oh, Effects of nitrogen on the mechanical properties of cold rolled TRIP-aided steel sheets, ISIJ Int. 46 (2006) 599-605.

[2] E. Girault, A. Mertens, P. Jacques, Y. Houbaert, B. Verlinden, J. Van Humbeeck, Comparison of the effects of silicon and aluminium on the tensile behaviour of multiphase TRIP-assisted steels, Scr. Mater. 44 (2001) 885-892

[3] O. Grassel, L. Kruger, G. Frommeyer, L. W. Meyer, High strength Fe-Mn-(Al, Si) TRIP/TWIP steels development - properties – application, Int. J. Plast. 16 (2000) 1391-1409.

[4] B. Mintz, W. D. Gunawardana, H. Su, Al as a solid solution hardener in Steels, Mater. Sci. and Technol. 24 (2008) 596-601.

[5] K. R. Kinsman, H. I. Aaronson, Influence of aluminum, cobalt, and silicon upon the kinetics of the proeutectoid ferrite reaction, Metall. Trans. 4 (1973) 959-967.

[6] H. Mabuchi, H. Nakao, The Effects of Excess Aluminum on Low-temperature Toughness in A302C Steels, ISIJ Int. 7 (1981) 495-501.

[7] H. Mabuchi, H. Nakao, The Effects of Excess Aluminum on Mechanical Properties of Mn-Mo, Mn-Mo-Ni and Mn-Mo-Ni-Cr Steels with Regard to Solute Interactions, ISIJ Int. 6 (1983) 504-512.

[8] T. Nakayama, N. Honjou, Effect of aluminum and nitrogen on the magnetic properties of non-oriented semi-processed electrical steel sheet, J. Magn. Magn. Mater. 213 (2000) 87-95.

[9] W. C. Jeong, Role of aluminum in hot-rolled ultra-low-carbon Nb-interstitial-free steels, Metall. and Mater. Trans. A 37 (2006) 3737-3739.

[10] Y. Palizdar, A. J. Scott, R. C. Cochrane, R. Brydson, Understanding the effect of aluminium on microstructure in low level nitrogen steels, Mater. Sci. Technol. 25 (2009) 1243-1248.

[11] Y. Palizdar, R. C. Cochrane, R. Brydson, F. Bygrave, A. J. Scott, Understanding the role of aluminium in low level nitrogen steels via microstructural characterisation , Journal of Physics: Conference Series 126 (2008) 012019.

[12] R. C. Cochrane, unpublished research, Corus, UK.

[13] J. K. Mackenzie, 2nd Paper on Statistics Associated with the Random Disorientation of Cubes, Biometrika 45 (1958) 229-240.

[14] F. G. Wilson, T. Gladman, Aluminum Nitride in Steel, Int. Mater. Rev. 33 (1988) 221-288.

[15] A. Saxena, S. K. Chaudhuri, Correlating the aluminum content with ferrite grain size and core loss in non-oriented electrical steel, ISIJ Int. 44 (2004) 1273-1275.

[16] A. Saxena, A. Sengupta, S. K. Chaudhuri, Effect of absorbed nitrogen on the microstructure and core loss property of non-oriented electrical steel, ISIJ Int. 45 (2005) 299-301.

[17] MTDATA, The NPL Software tool for the calculation of phase equilibria and thermodynamic properties, National Physical Laboratory, UK.

[18] R. Bengochea, B. Lopez, I. Gutierrez, Influence of the prior austenite microstructure on the transformation products obtained for C-Mn-Nb steels after continuous cooling, ISIJ Int. 39 (1999) 583-591.

[19] W. B. C. Morrison, J. A., Controlled rolling, in: Br. Steel Corp., Open [Rep.], Br. Steel, Sheffield (1975) 20-29.

[20] F. Vodopivec, M. Gabrovsek, M. Kmetic, A. Rodic, Interpass Recrystallization of Austenite in Some Steels During Rolling, Met. Technol. 11 (1984) 481-488.

[21] R. Priestner, A. K. Ibraheem, Processing of steel for ultrafine ferrite grain structures, in: Materials Congress 2000, I O M Communications Ltd Inst Materials, Cirencester, England, 2000, pp. 1267-1272.

[22] B. Eghbali, EBSD study on the formation of fine ferrite grains in plain carbon steel during warm deformation, Mater. Lett. 61 (2007) 4006-4010.

Table 1 Steel compositions (wt%), excess Al based on equation (1) and rolling treatments

| Steel sample | C | Si | Mn | P | S | Al | N | Aluminium (free) | Rolling schedules |
|---|---|---|---|---|---|---|---|---|---|
| E | 0.028 | 0.28 | 1.41 | 0.001 | 0.001 | 0.02 | 0.001 | 0.018 | |
| F | 0.019 | 0.28 | 1.41 | 0.001 | 0.001 | 0.48 | 0.001 | 0.478 | HR |
| G | 0.022 | 0.29 | 1.41 | 0.001 | 0.001 | 0.94 | 0.001 | 0.938 | |
| L | 0.028 | 0.28 | 1.41 | 0.001 | 0.001 | 0.02 | 0.001 | 0.018 | CR |
| M | 0.019 | 0.28 | 1.41 | 0.001 | 0.001 | 0.48 | 0.001 | 0.478 | |

Table 2 The rolling schedule for HR. In the case of CR, the slab was held at Pass 7* allowed to reach a nominal temperature of 1080 $^{o}$C and then rolled as the same as HR (see text).

| Pass number | Plate thickness (mm) | | Reduction (%) | Nominal temperature for HR ($^{o}$C) |
|---|---|---|---|---|
| | Start | Finish | | |
| 1 | 100 | 95 | 5.0 | 1250 |
| 2 | 95 | 80 | 15.7 | |
| 3 | 80 | 70 | 12.5 | |
| 4 | 70 | 60 | 14.3 | |
| 5 | 60 | 50 | 16.7 | |
| 6 | 50 | 42 | 16.0 | 1200 |
| 7* | 42* | 35 | 16.7 | |
| 8 | 35 | 28 | 20.0 | 1160 |
| 9 | 28 | 23 | 17.8 | |
| 10 | 23 | 19 | 17.4 | |
| 11 | 19 | 13 | 31.6 | 1095 |

Table(s)

Table 3 Ferrite grain size determined by EBSD.

| Rolling schedule | Steel | ASTM number | Mean linear Intercept (μm) |
|---|---|---|---|
| HR | E | 7.1 | 27.1 |
| | F | 7.2 | 26.5 |
| | G | 8.4 | 17.3 |
| CR | L | 6.4 | 35.5 |
| | M | 9.5 | 11.8 |

Table 4. Critical no-partition transformation temperatures $Ae_1$, $Ae_3$ as predicted by MTData thermodynamic software

| Steel | $Ae_1$ (ºC) | $Ae_3$ (ºC) |
|---|---|---|
| E | 679 | 859 |
| F | 691 | 923 |
| G | 709 | 1053 |

Table 5 Correlation between the amount of low angle grain boundaries and difference between $Ae_3$ and FRT for each steel

| Steel | Difference between $Ae_3$ and FRT (ºC) | The amounts of low angle grain boundaries below 15º (%) |
|---|---|---|
| E | 240 | 5.7 |
| F | 177 | 5.8 |
| G | 50 | 10 |
| L | 90 | 8.9 |
| M | 27 | 12.4 |

FIGURE 1

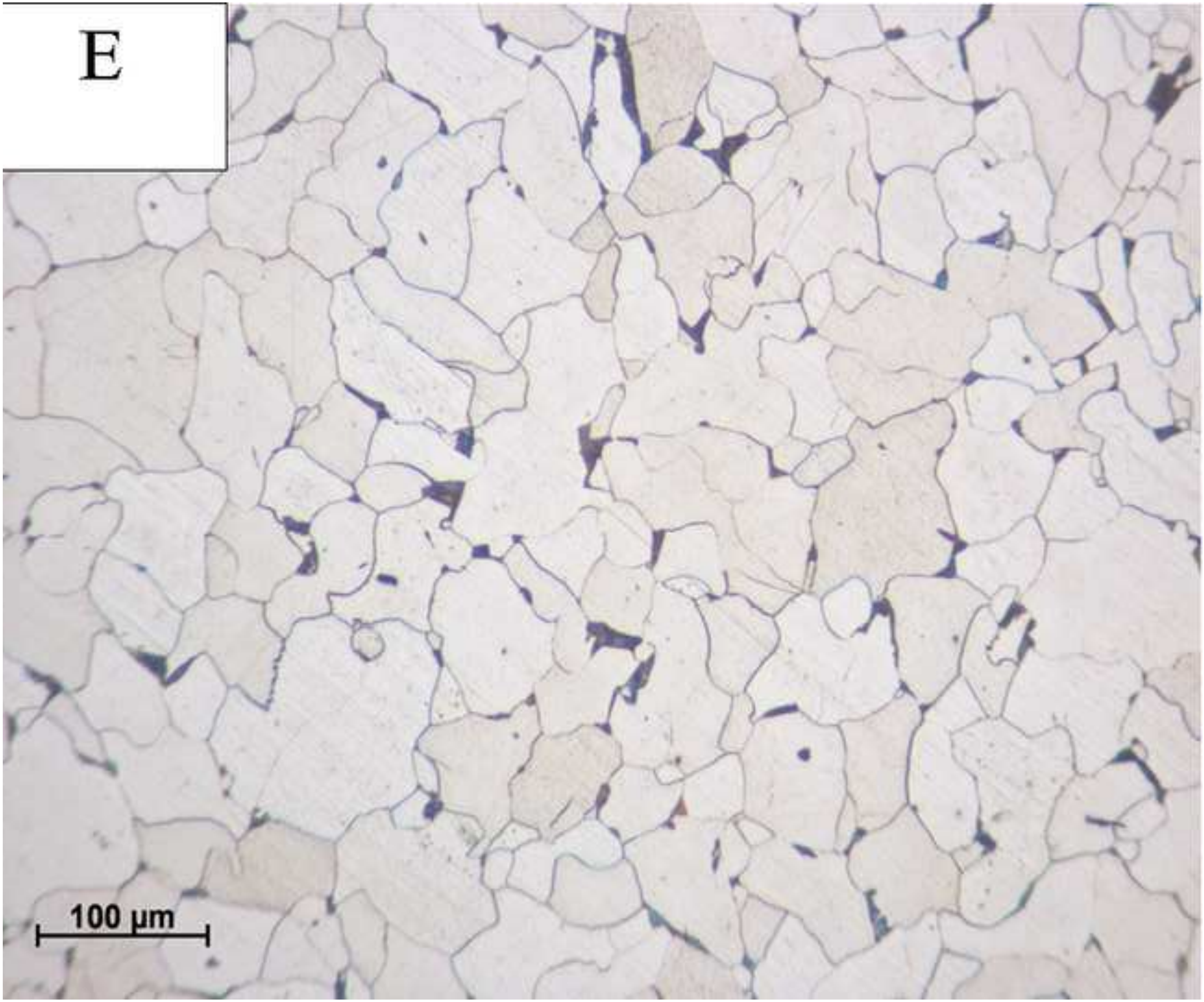

FIGURE 1

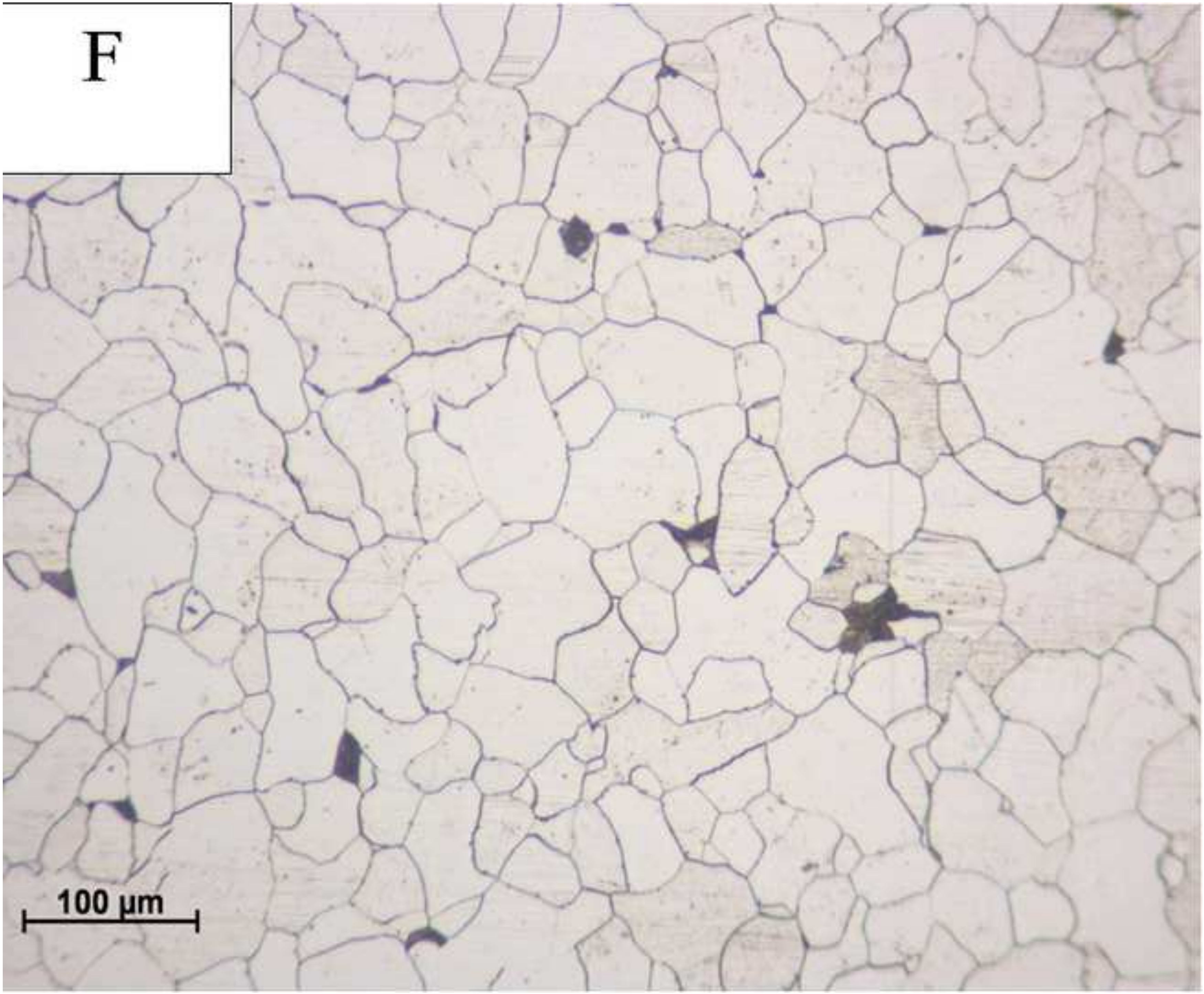

FIGURE 1

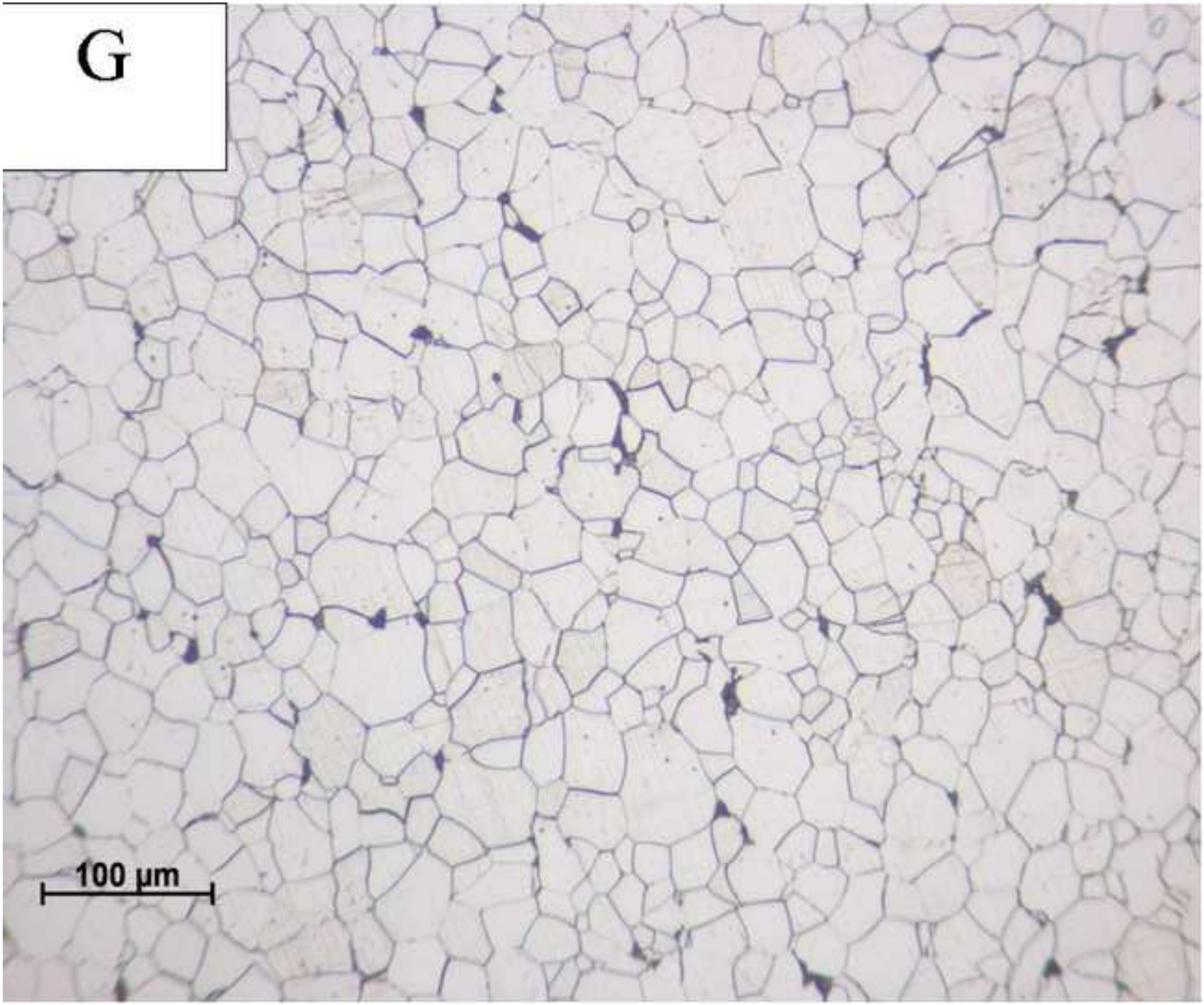

FIGURE 1

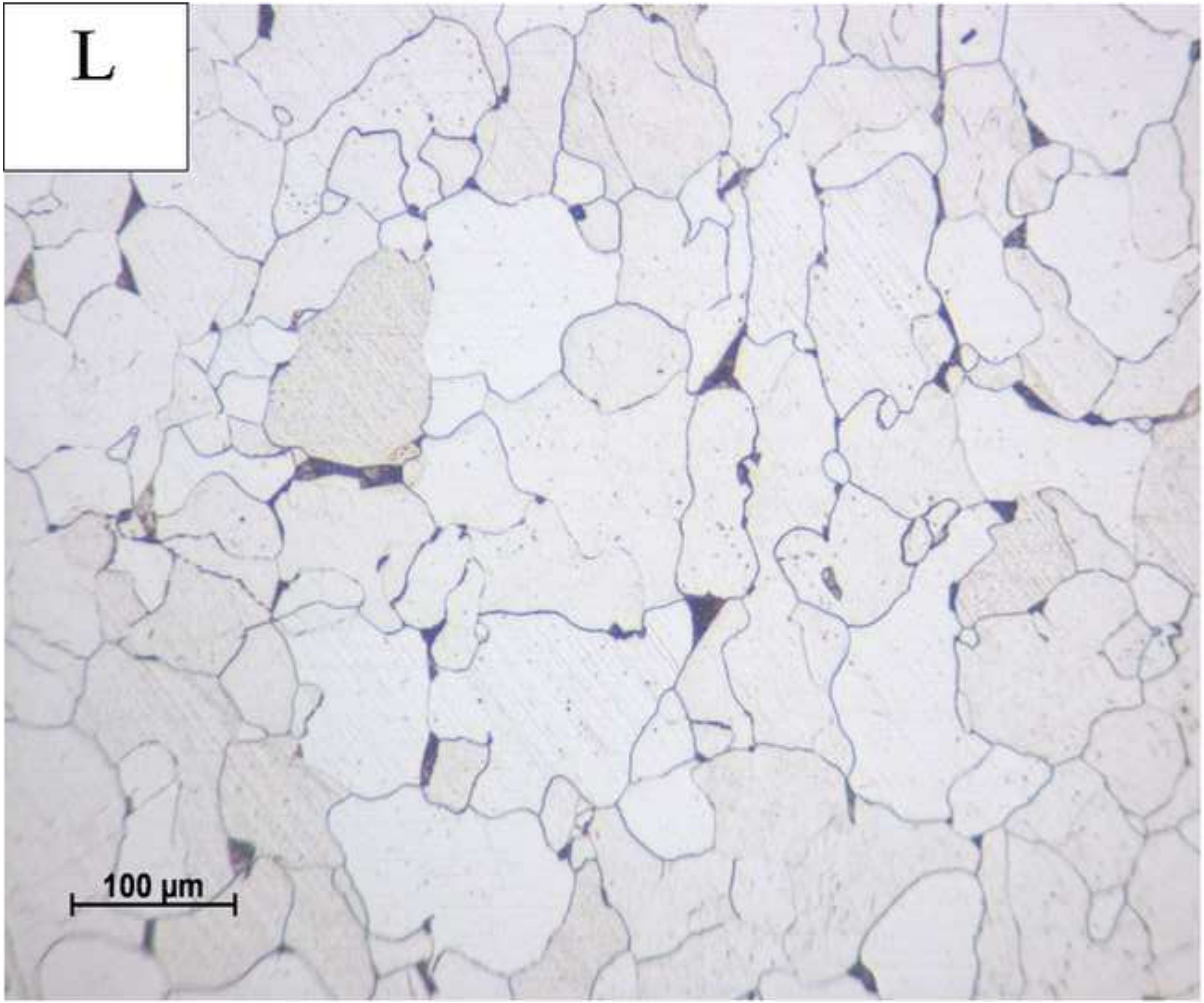

FIGURE 1

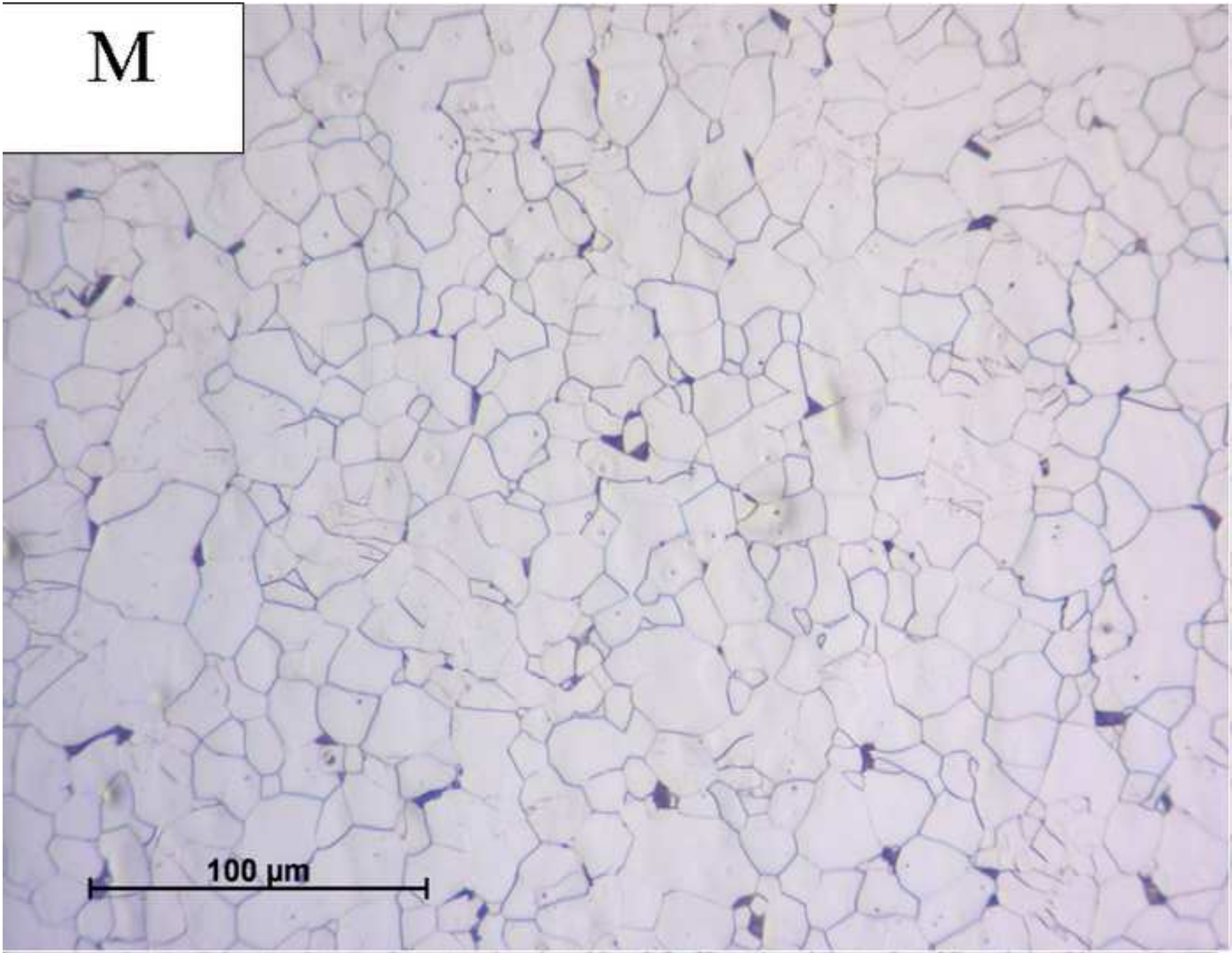

FIGURE 2

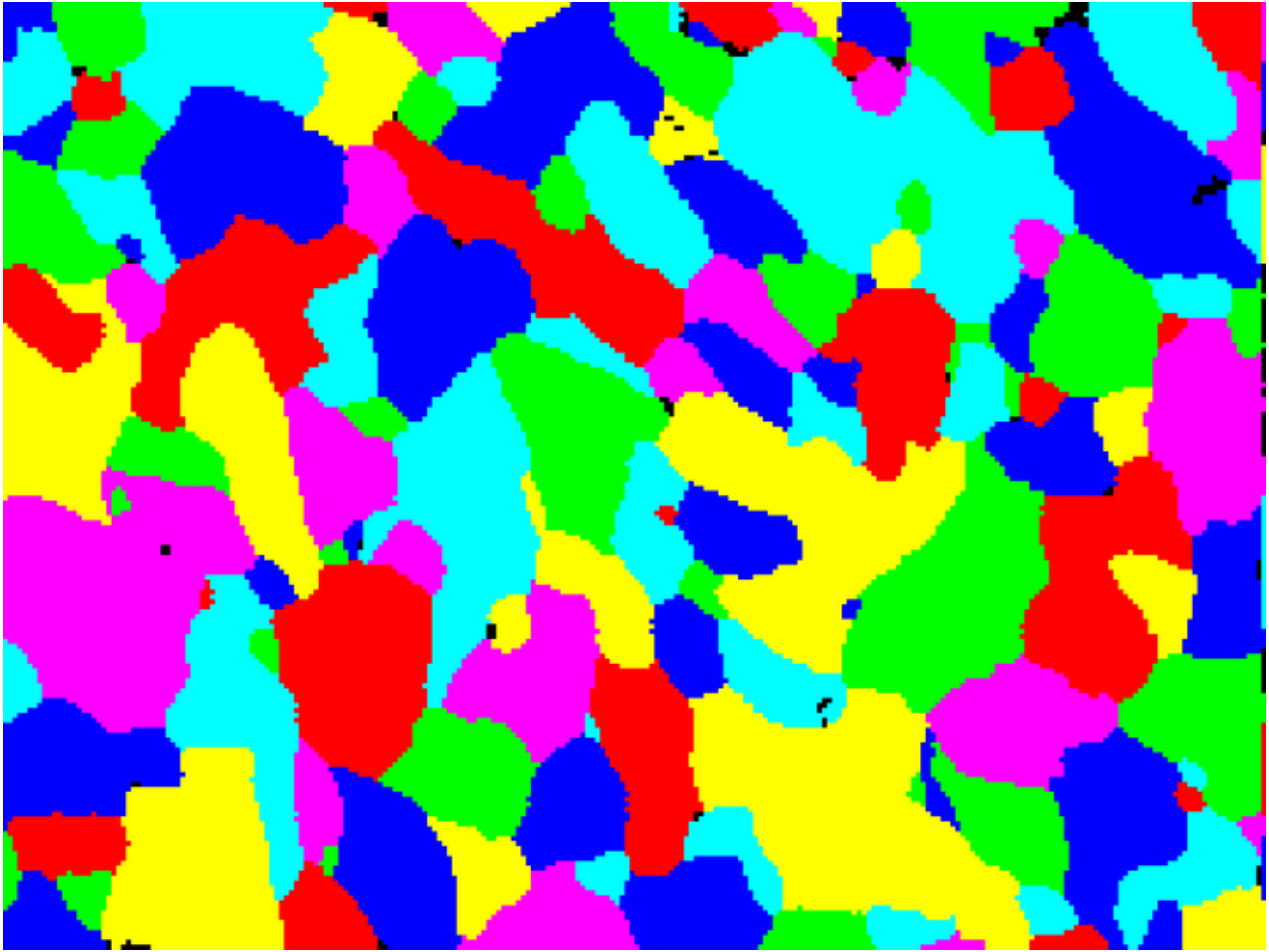

FIGURE 2

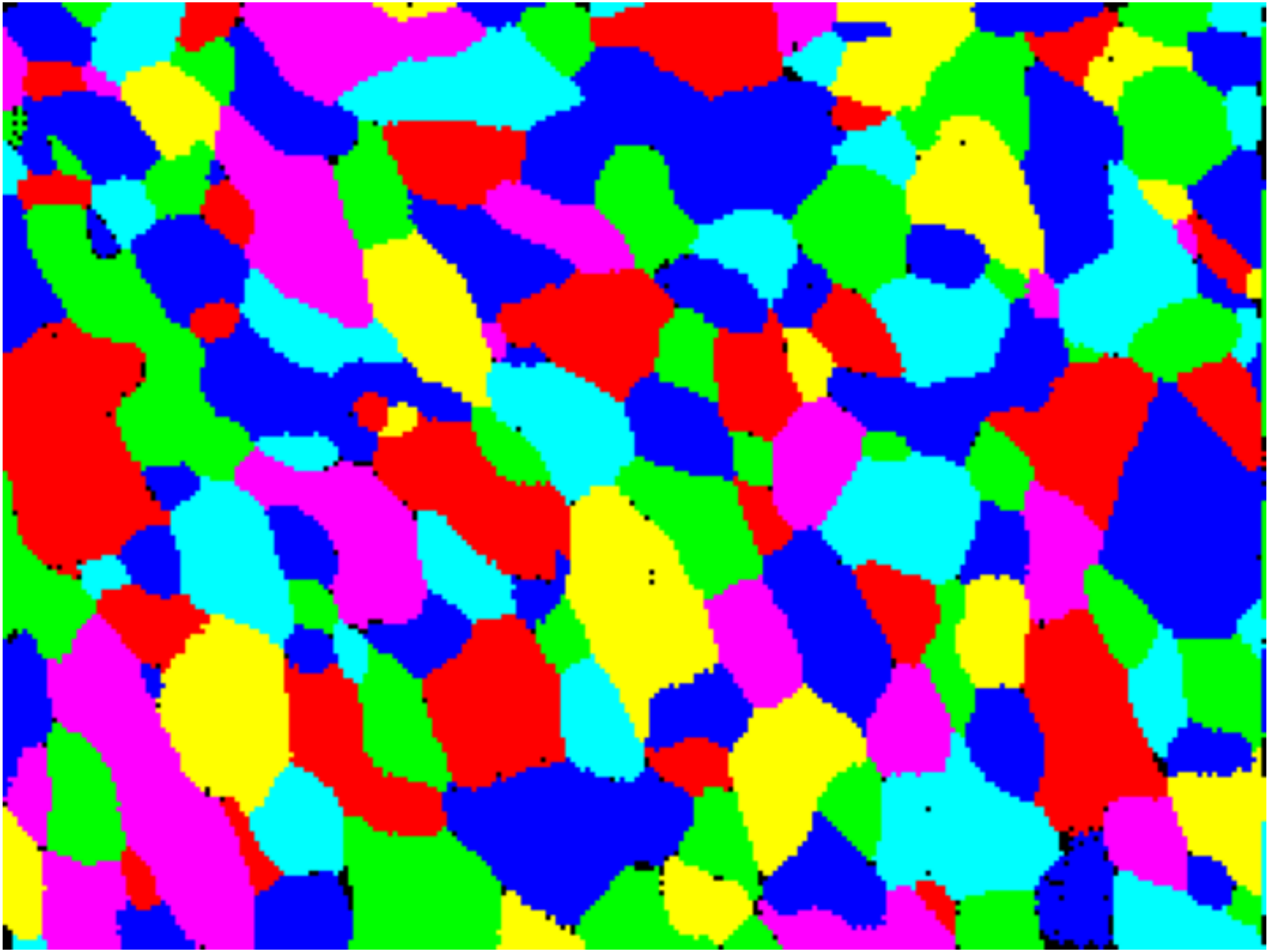

FIGURE 2

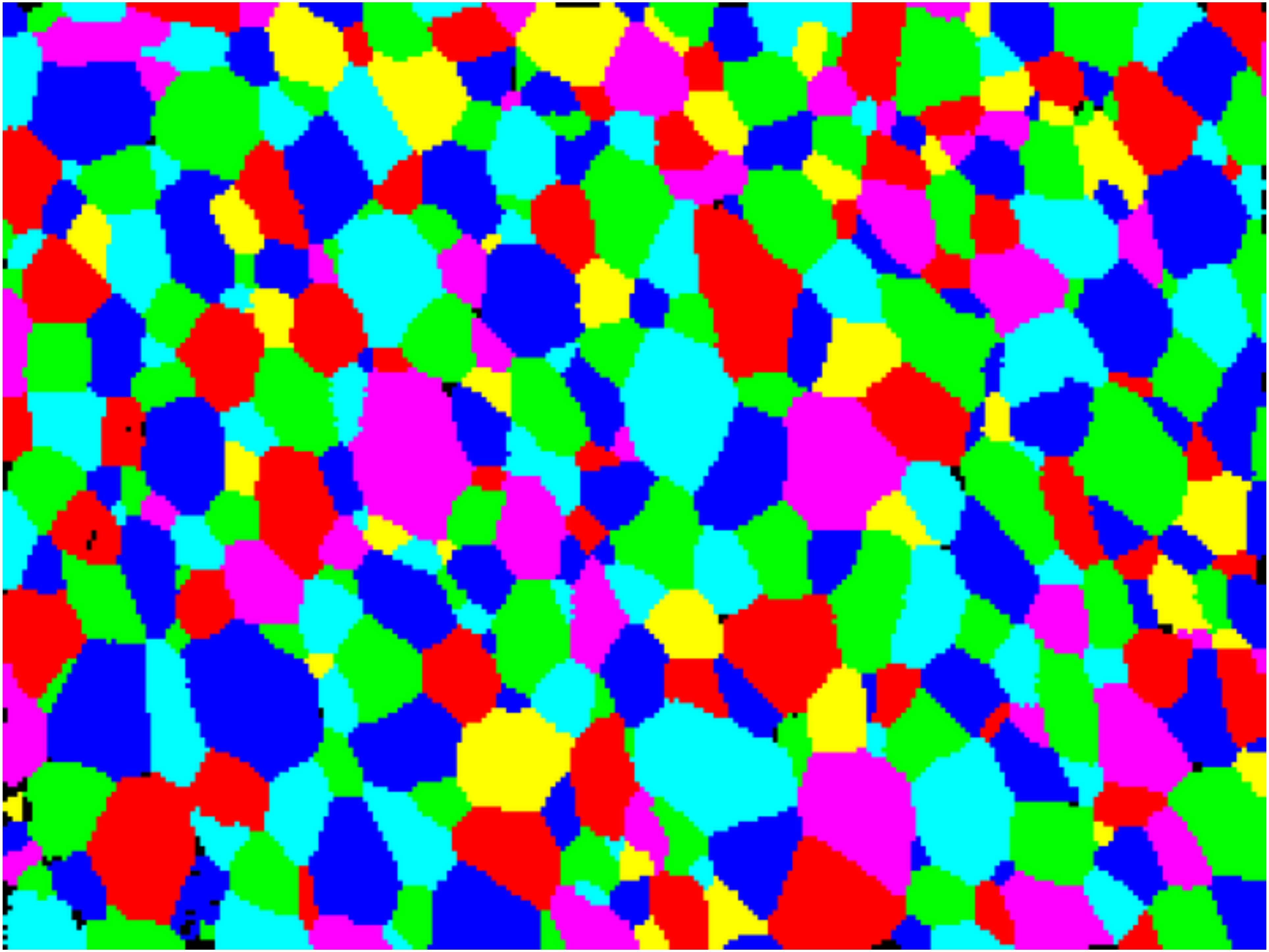

FIGURE 2

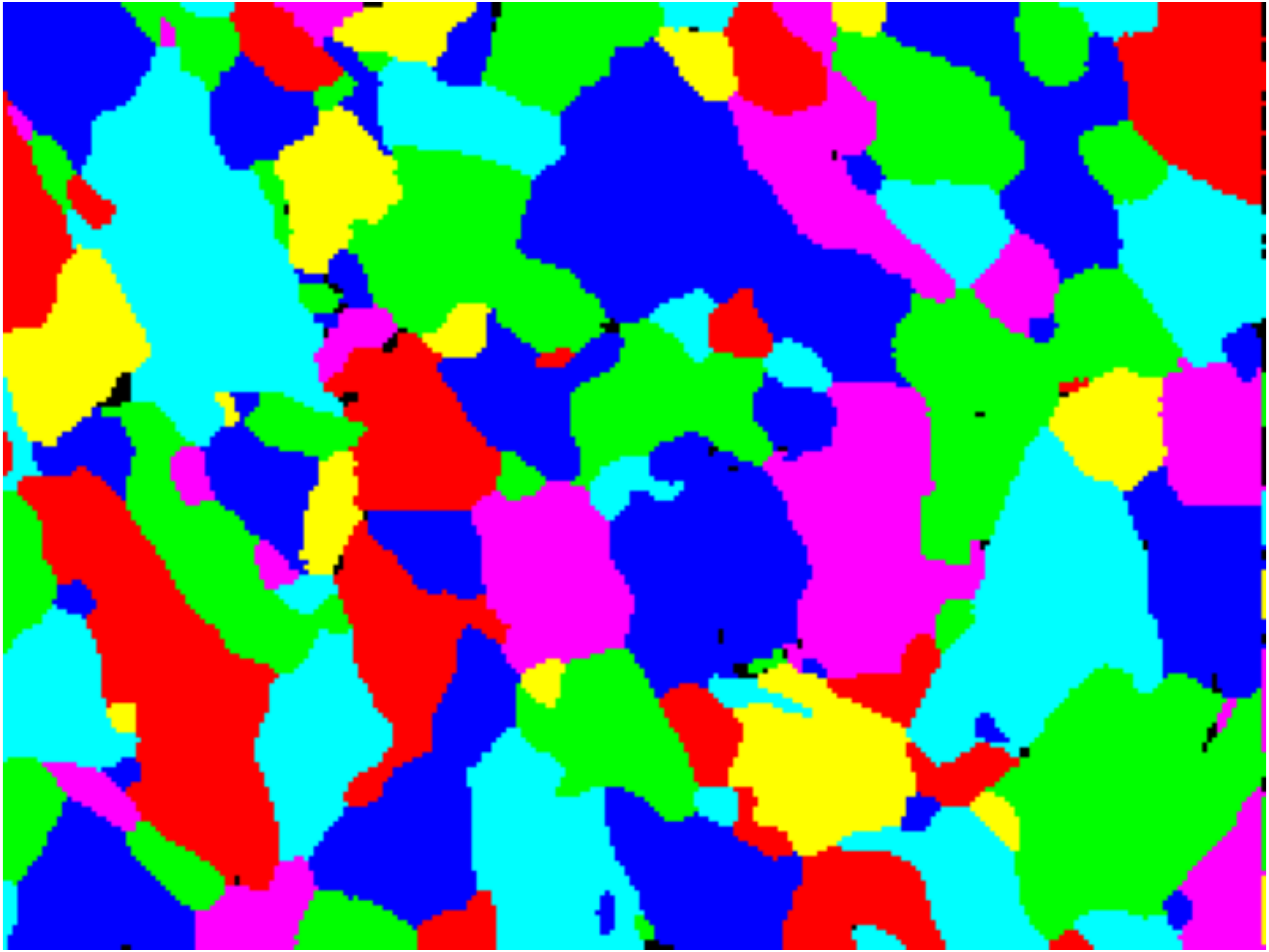

**FIGURE 2**

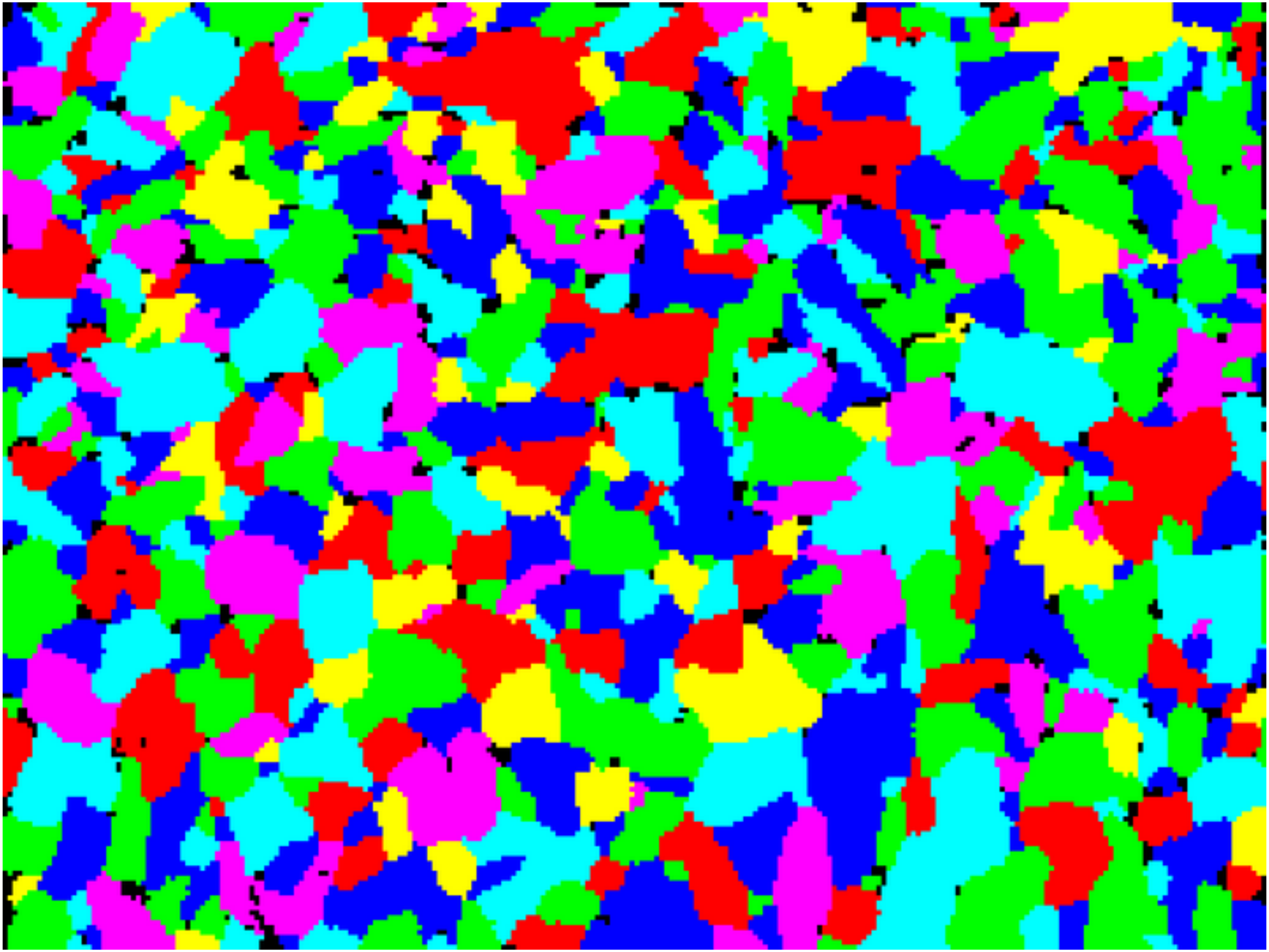

FIGURE 3a

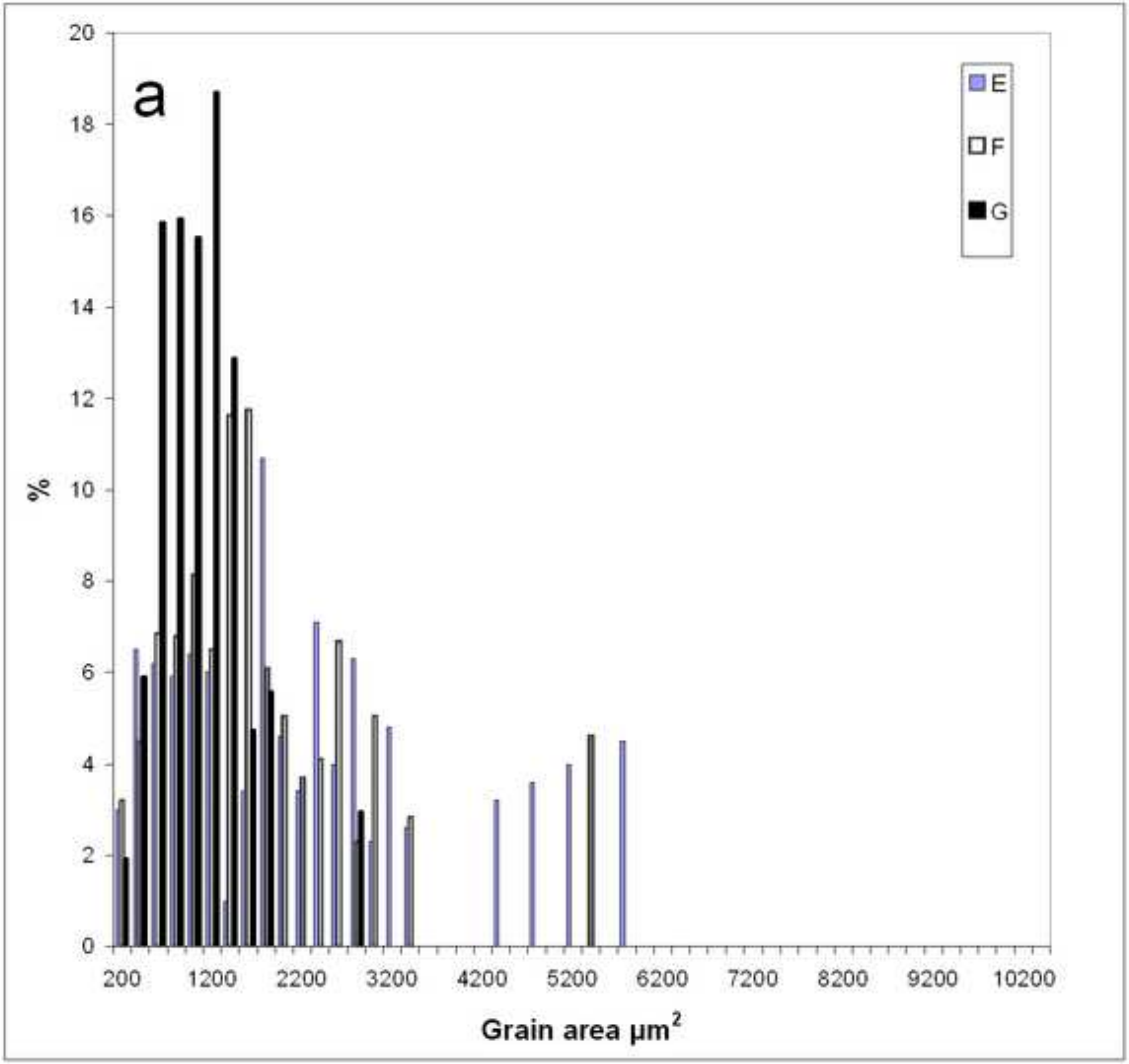

a
E
F
G
%
20
18
16
14
12
10
8
6
4
2
0
200
1200
2200
3200
4200
5200
6200
7200
8200
9200
10200
Grain area μm2

**FIGURE 3b**

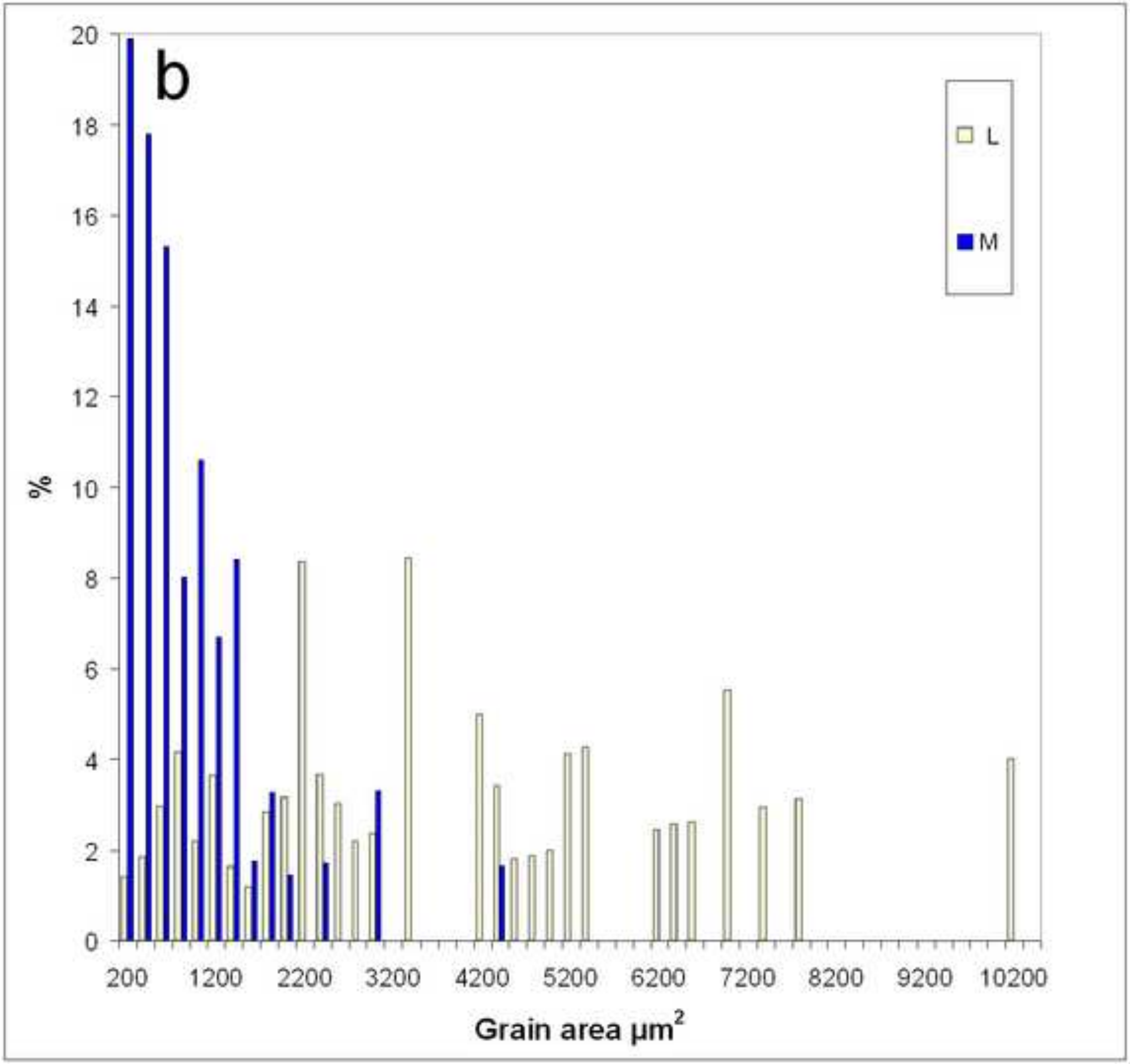

b
L
M
%
20
18
16
14
12
10
8
6
4
2
0
200
1200
2200
3200
4200
5200
6200
7200
8200
9200
10200
Grain area µm²

**FIGURE 4a**

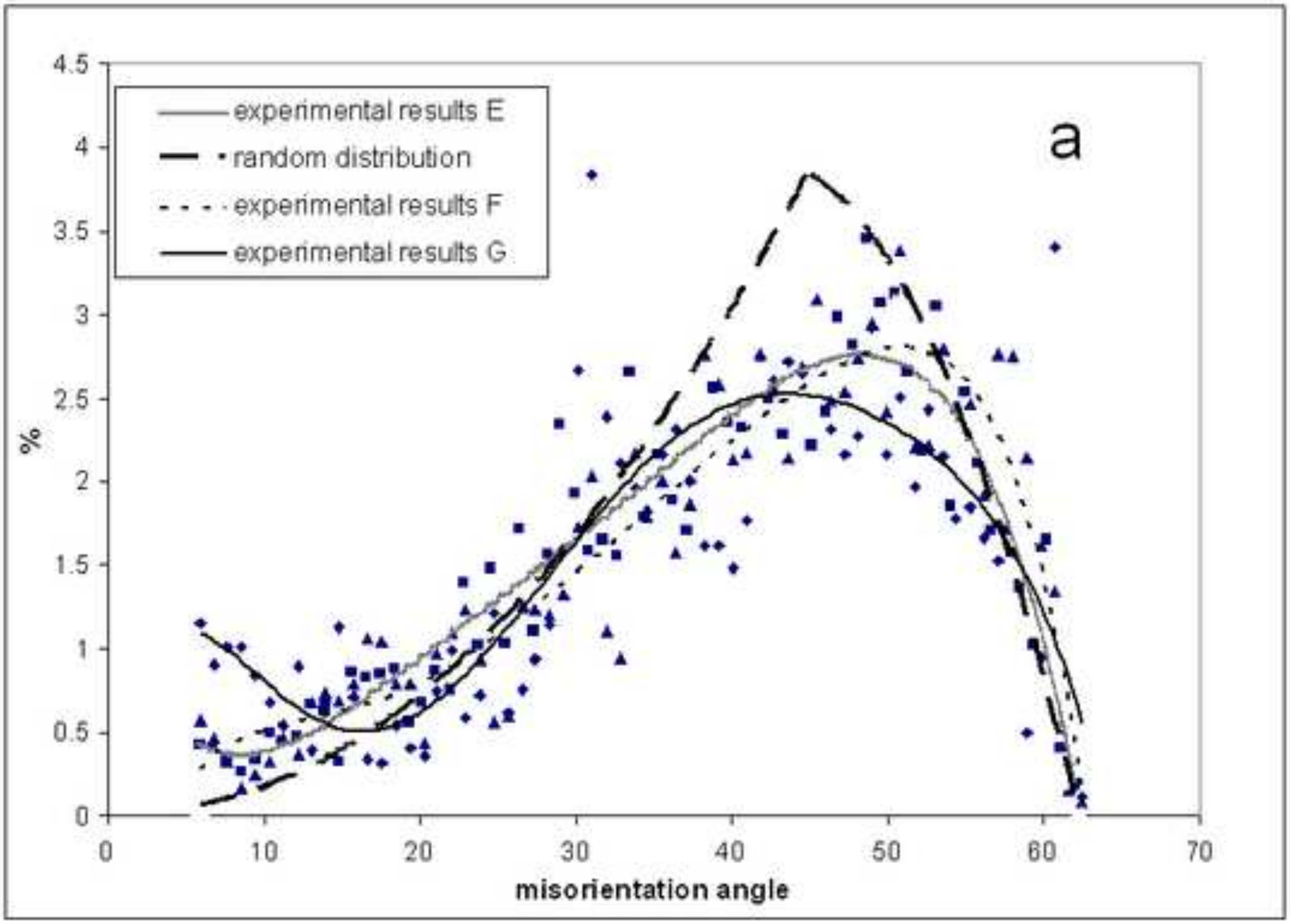
experimental results E
random distribution
experimental results F
experimental results G
a
%
misorientation angle
4.5
4
3.5
3
2.5
2
1.5
1
0.5
0
0
10
20
30
40
50
60
70

**FIGURE 4b**

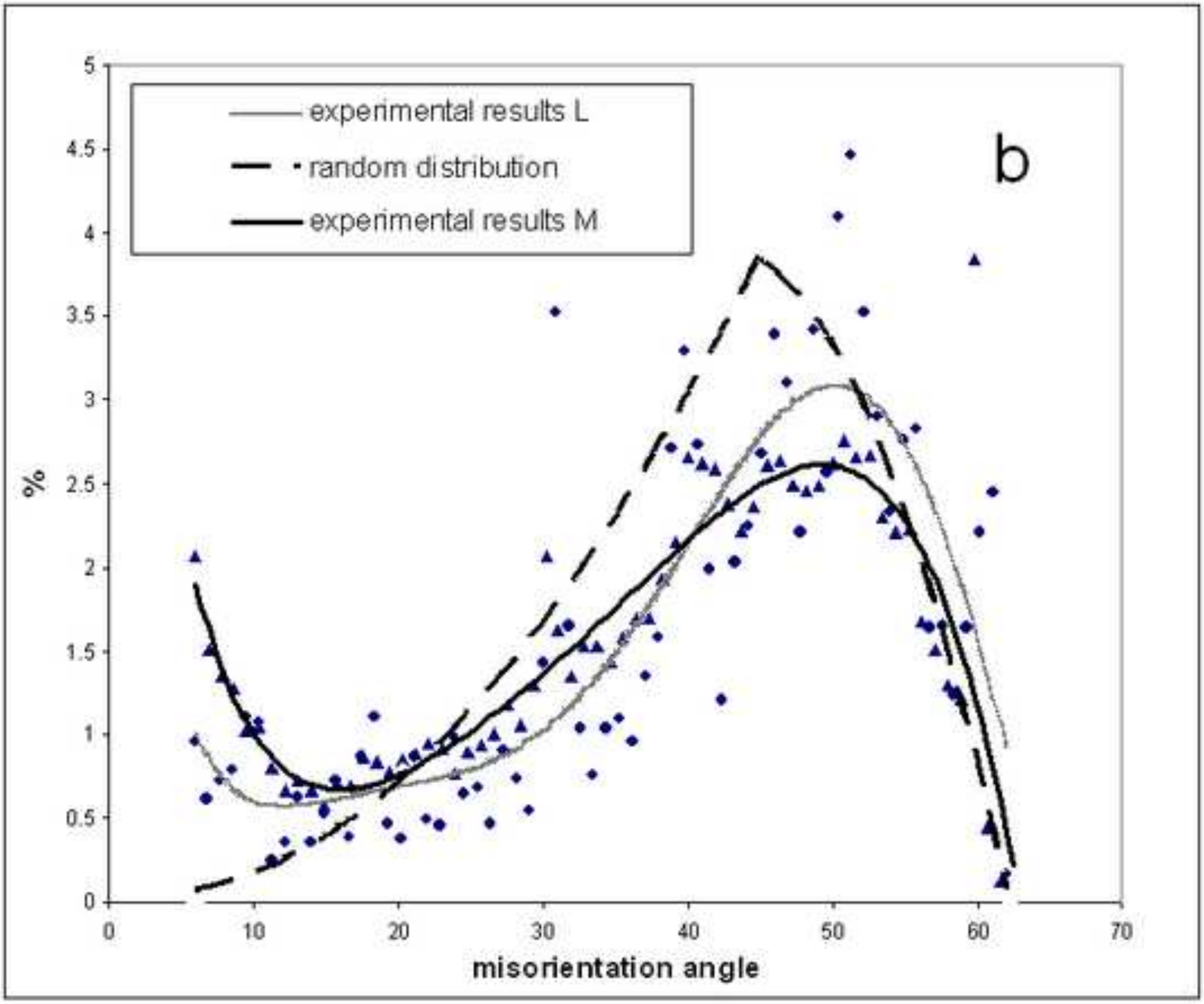

experimental results L
random distribution
experimental results M
b
%
misorientation angle
0
0.5
1
1.5
2
2.5
3
3.5
4
4.5
5
0
10
20
30
40
50
60
70

FIGURE 5a

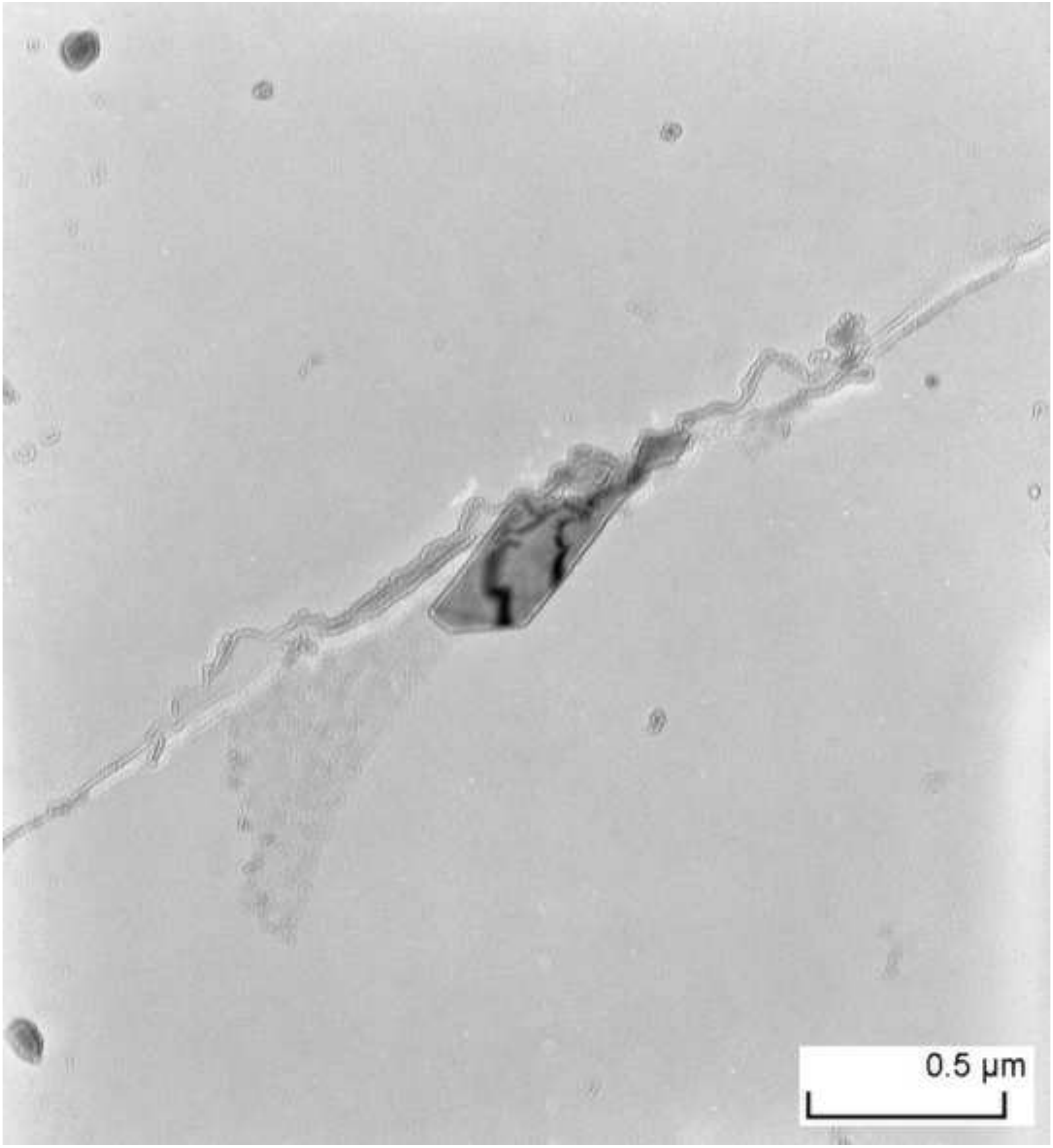

**FIGURE 5b**

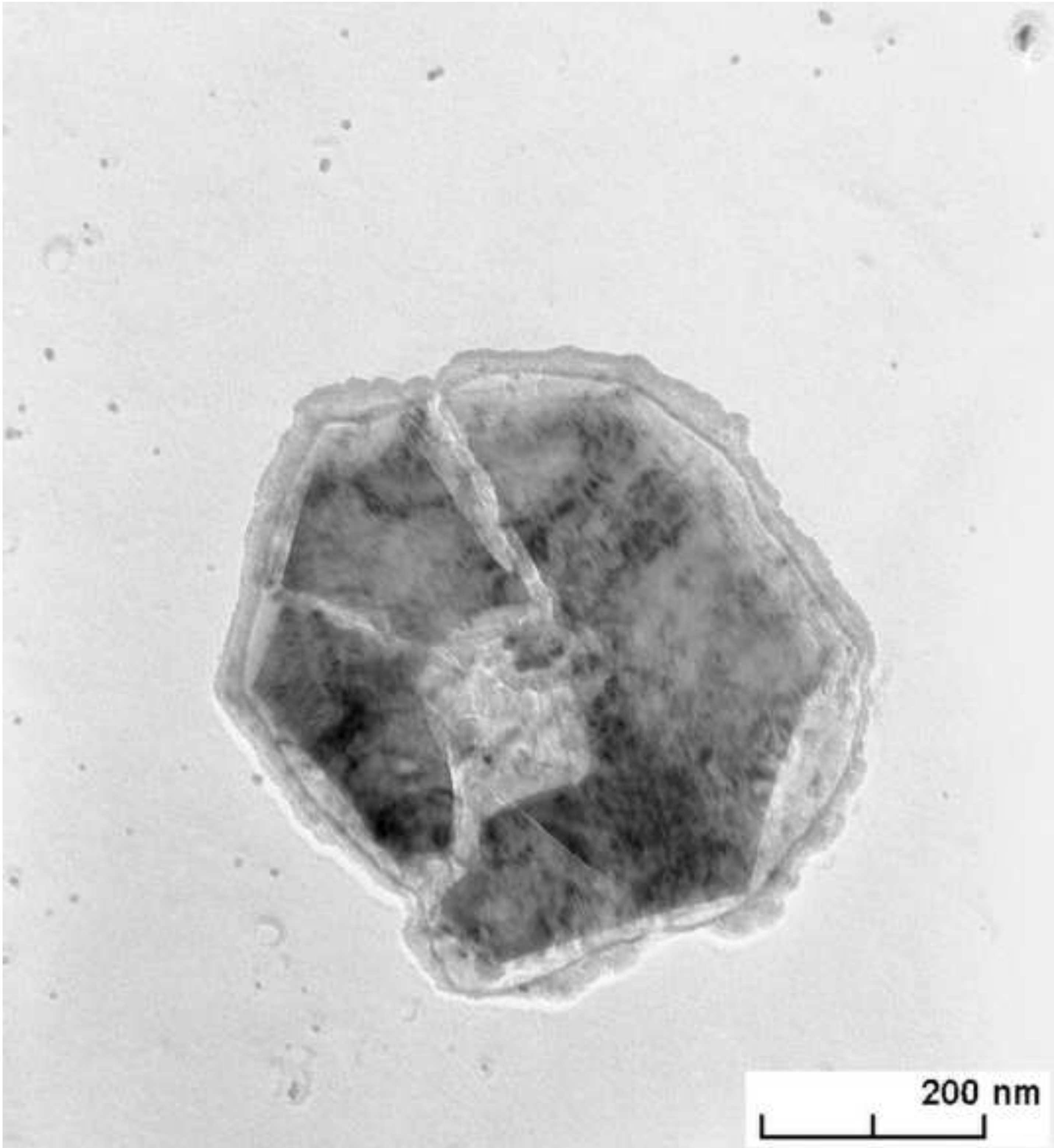

**FIGURE 6**

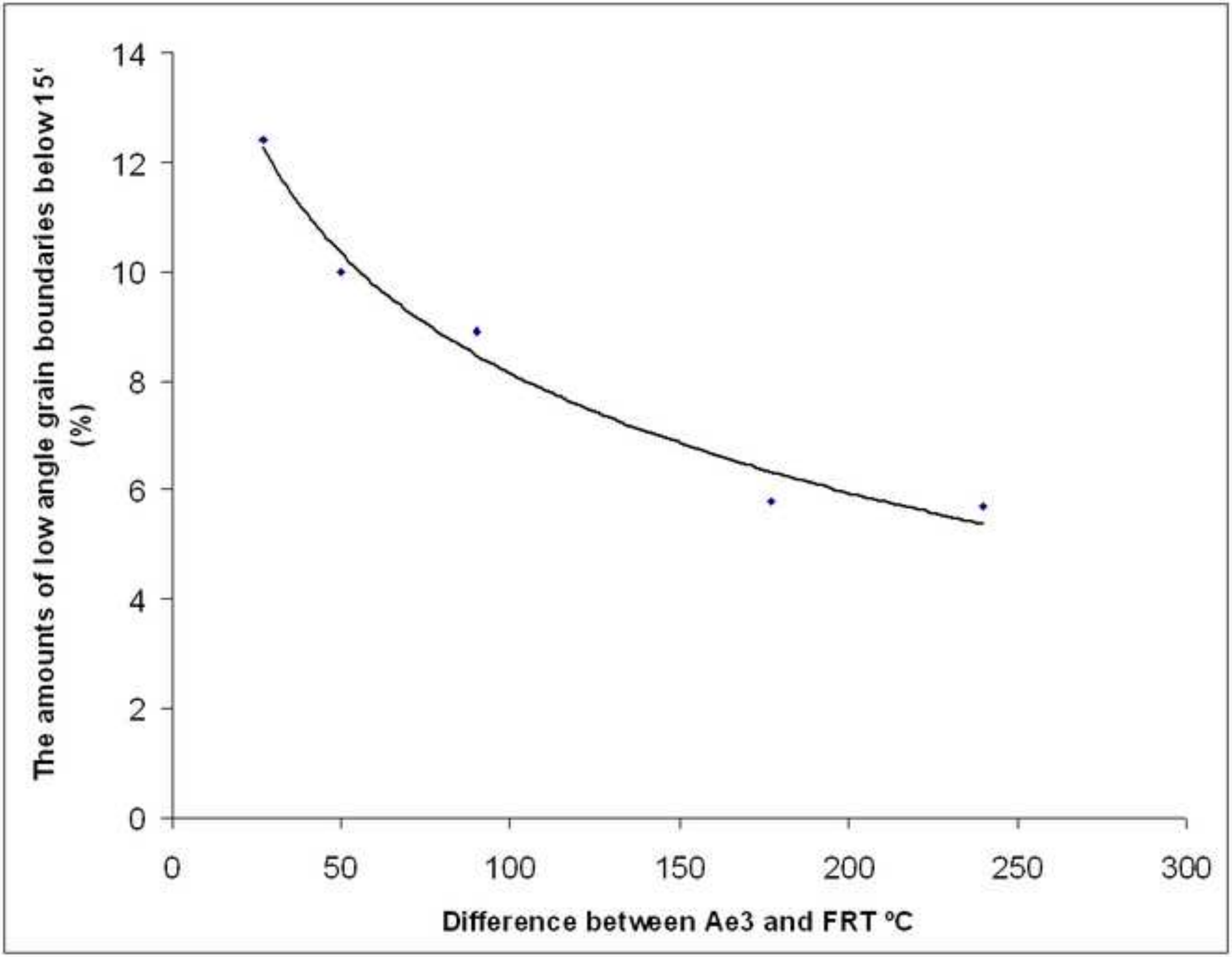

14
12
10
8
6
4
2
0
0
50
100
150
200
250
300
The amounts of low angle grain boundaries below15°
(%)
Difference between Ae3 and FRT °C